

Visualizing class specific heterogeneous tendencies in categorical data

Mariko Takagishi

Graduate School of Culture and Information Science, Doshisha University
and

Michel van de Velden

Department of Econometrics, Erasmus University Rotterdam

November 6, 2018

Abstract

In multiple correspondence analysis, both individuals (observations) and categories can be represented in a biplot. In this biplot, relationships between categories, between individuals, as well as the associations between individuals and categories, are depicted jointly. It can be useful to add information regarding the individuals to enhance interpretation. Such additional information can consist, for example, of a set of categorical variables for which the interdependencies are not of immediate concern, but that might assist in interpreting the plot, and in particular, with respect to the relationships between individuals and categories. In this paper, we propose a new method for adding such additional information. We introduce a multiple set cluster correspondence analysis approach that finds clusters specific for classes, defined as subsets of the data corresponding to the categories of the additional variables. Our method can be used to construct a biplot that visualizes heterogeneous tendencies of the individuals, as well as their relationship with respect to the original categorical variables. We investigate the performance of the proposed method through a simulation study and we apply it to a data set regarding road accidents in the United Kingdom.

Keywords: Multiple Correspondence Analysis, Clustering, Visualization, External Information, Supplementary Variable, Contingency Table.

1 Introduction

Correspondence analysis (CA) and multiple correspondence analysis (MCA) are popular methods for visually interpreting associations among categorical variables. In MCA, quantifications for categories and individuals can be obtained and depicted in a biplot. A biplot aims to visualize associations between categories and between individuals, as well as identifying associations between individuals and categories (e.g., M. Greenacre, 1993; Gower & Hand, 1996). In the MCA biplot, if many individuals choose the same two categories, quantifications for these categories and the corresponding individuals, tend to be located close to each other. Hence, using an MCA biplot, we can visually identify individuals with similar tendencies in choosing categories.

The addition of pertinent external information regarding individuals can be useful in enhancing the interpretation of the MCA biplot. By external information, we mean information that we do not want to use for the estimation of the coordinates, but that may be useful for interpretation of the biplot.

There have been several studies regarding the incorporation of external information regarding individuals in an MCA biplot (e.g., Yanai, 1986, 1988; Böckenholt & Böckenholt, 1990; Takane, Yanai, & Mayekawa, 1991; Van Buuren & de Leeuw, 1992; Böckenholt & Takane, 1994; Yanai & Maeda, 2002). Takane and Hwang (2002) showed that various objectives incorporating the external information can be generalized into a linear constraint framework. Here, we only consider external information that consists of a set of categorical variables. Furthermore, we shall refer to the subsets of the data that correspond to categories of the external information as classes. We aim to visually interpret how tendencies of individuals differ depending on these classes.

One way to achieve our objective, is by including the external variables before applying MCA. However, when this is done, the information is no longer external and becomes a part of the original analysis. An alternative approach is to color individual quantifications (i.e., points) according to the classes. For example, if gender is considered to be an external variable, the points corresponding to males can be colored black, while those corresponding to females are colored red. With this approach, we can only incorporate external information corresponding to one categorical variable at the time. Alternatively, one can obtain average quantification for each class. Then, by plotting these average points, as well as the category points of the original (non-external) variables, we can see the relationship between the external information and the categories. We shall refer to this as “averaging approach”.

In the averaging approach, however, one only finds average tendencies of many individuals within a class. Heterogeneous tendencies within a class remain unobserved. Hence, when there is a relatively small group in a class that has a strong tendency towards a particular category that is not selected by the majority, this would not be visible in the biplot when the averaging approach is used. Nevertheless, such tendencies could be interesting to interpret if we want to characterize tendencies by class.

In this paper, we propose a new approach that finds class specific clusters and depicts these clusters together with the categories of the (original) variables. This results in a visualization of the categories (i.e., the category quantifications) together with points

representing different clusters for the different classes of data. Moreover, it enables us to visualize different heterogeneous tendencies within a class in a single MCA biplot, and in addition, to visualize the relationships among classes corresponding to the categories of different external variables.

The remainder of this paper is organized as follows. In Section 2, we introduce our proposed method and show its relationship to existing approaches, including the linear row constraint framework. In Section 3, we compare a biplot obtained using the averaging approach and one obtained using our proposed method. Then, in Section 4, we appraise our method under different scenarios concerning the external information, using a simulation study. We illustrate our method by applying it to empirical data in Section 5.

2 Multiple Set Cluster CA

In this section, we introduce our approach, which we call multiple set cluster CA (MSCCA). Furthermore, we show the relationship of MSCCA to several existing methods, such as cluster CA (van de Velden, D’Enza, & Palumbo, 2017), CA, and the linear row constraint framework.

2.1 The MSCCA objective function

Suppose that we have N observations on m categorical variables, and in conjunction, that, for the same N observations, we have H additional categorical variables containing external information. Henceforth, we refer to these H additional variables as supplementary variables. In order to formulate the MSCCA objective function, some notation is required.

Let q_j ($j = 1, \dots, m$) be the number of categories for the j th variable and let $Q = \sum_{j=1}^m q_j$. We create dummy matrices \mathbf{Z}_j for the m categorical variables using given categorical data. That is, the rows of \mathbf{Z}_j are $(q_j \times 1)$ vectors $\mathbf{z}_{ji} = (z_{jil})$ ($i = 1, \dots, n$; $\ell = 1, \dots, q_j$), where $z_{jil} = 1$ if individual i chooses the ℓ th category in the j th variable, and the other elements are 0. Similarly, we create dummy matrices for the H supplementary variables, with $\mathbf{V}_h = (v_{his})$, ($h = 1, \dots, H$; $s = 1, \dots, r_h$), where r_h is the number of categories for the h th supplementary variable.

In addition, let K_{hs} be the number of clusters for the s th category (class) of the h th supplementary variable, with $K_h = \sum_{s=1}^{r_h} K_{hs}$. Let \mathbf{B}_j be the $q_j \times p$ quantification matrix for the categories of the j th variable, where p denotes the number of dimensions, and let \mathbf{U}_h and \mathbf{G}_h be $N \times K_h$ cluster indicator matrices and $K_h \times p$ quantification matrices for cluster centers in the h th supplementary variable, respectively. The objective function of

MSCCA can be defined as

$$\min_{\mathbf{U}_h, \mathbf{G}_h, \mathbf{B}_j} \phi(\mathbf{U}_h, \mathbf{G}_h, \mathbf{B}_j | \mathbf{Z}_j, \mathbf{V}_h) = \frac{1}{NHm} \sum_{j=1}^m \sum_{h=1}^H \|\mathbf{U}_h \mathbf{G}_h - \mathbf{Z}_j \mathbf{B}_j\|^2 \quad (1)$$

$$\text{s.t.} \quad \frac{1}{Nm} \sum_{j=1}^m \mathbf{B}_j' \mathbf{Z}_j' \mathbf{Z}_j \mathbf{B}_j = \mathbf{I}_p, \quad \mathbf{J}_N \mathbf{U}_h \mathbf{G}_h = \mathbf{U}_h \mathbf{G}_h$$

$$\text{where } \mathbf{U}_h = \begin{pmatrix} \mathbf{u}'_{h11} & \cdots & \mathbf{u}'_{h1r_h} \\ \vdots & \ddots & \vdots \\ \mathbf{u}'_{hN1} & \cdots & \mathbf{u}'_{hNr_h} \end{pmatrix}$$

$$\mathbf{u}_{his} = (u_{his1}, \dots, u_{hisK_{hs}})'$$

$$\text{s.t.} \quad \begin{cases} u_{hisk} \in \{0, 1\}, & (k = 1, \dots, K_{hs}), \quad \sum_{k=1}^{K_{hs}} u_{hisk} = 1 & (v_{his} = 1) \\ u_{hisk} = 0, & (k = 1, \dots, K_{hs}) & (v_{his} = 0) \end{cases} \quad (2)$$

$$(i = 1, \dots, n; s = 1, \dots, r_h; h = 1, \dots, H).$$

Here, $\mathbf{J}_N = \mathbf{I}_N - N^{-1} \mathbf{1}_N \mathbf{1}_N'$ is the centering matrix, where \mathbf{I}_N is an $N \times N$ identity matrix, and $\mathbf{1}_N$ is an $N \times 1$ vector of ones. Note that, when we estimate parameters, the number of clusters K_{hs} ($h = 1, \dots, H; s = 1, \dots, r_h$) must be pre-specified.

The constraint on \mathbf{U}_h in (2) defines a two level hierarchical cluster structure in the data. Specifically, for each supplementary variable h , the individuals are first divided into r_h *known* classes corresponding to the categories of the variable as indicated by $\mathbf{u}_{hi1}, \dots, \mathbf{u}_{hir_h}$. Then, within each class s (where $s = 1, \dots, r_h$), individuals are assigned to K_{hs} unknown clusters as indicated by $u_{his1}, \dots, u_{hisK_{hs}}$.

We illustrate the construction of \mathbf{U}_h using a small example. Suppose that we have 5 observations and that one supplementary variable, say h , corresponds to gender. In addition, assume we want to find two clusters for the males and one cluster for females, that is, $K_{h1} = 2$ and $K_{h2} = 1$. Let observations $i = 1, 3, 5$ be males where $i = 1, 3$ are in the first male cluster and $i = 5$ is in the second one, individuals $i = 2, 4$ are females.

First, consider the cluster indicator vector for individual $i = 1$, \mathbf{u}_{h1} . Since we partition the data by gender, the vector is split as $\mathbf{u}'_{h1} = (\mathbf{u}'_{h11}, \mathbf{u}'_{h12})$, where \mathbf{u}_{h11} and \mathbf{u}_{h12} denote the cluster indicator vectors of individual i in the male and female class, respectively. Doing this for all individuals, we obtain

$$\mathbf{U}_h = \begin{pmatrix} \mathbf{u}'_{h11} & \mathbf{u}'_{h12} \\ \mathbf{u}'_{h21} & \mathbf{u}'_{h22} \\ \mathbf{u}'_{h31} & \mathbf{u}'_{h32} \\ \mathbf{u}'_{h41} & \mathbf{u}'_{h42} \\ \mathbf{u}'_{h51} & \mathbf{u}'_{h52} \end{pmatrix} = \begin{pmatrix} 1 & 0 & 0 \\ 0 & 0 & 1 \\ 1 & 0 & 0 \\ 0 & 0 & 1 \\ 0 & 1 & 0 \end{pmatrix}.$$

To relate our method to other methods, (1) can be rewritten as

$$\min_{\mathbf{U}, \mathbf{G}, \mathbf{B}} \phi(\mathbf{U}, \mathbf{G}, \mathbf{B} | \mathbf{Z}, \mathbf{V}) = \frac{1}{NHm} \sum_{j=1}^m \|\mathbf{U}\mathbf{G} - \mathbf{Z}_j^H \mathbf{B}_j\|^2 \quad (3)$$

$$\text{s.t.} \quad \frac{1}{Nm} \sum_{j=1}^m \mathbf{B}_j' \mathbf{Z}_j^{H'} \mathbf{Z}_j^H \mathbf{B}_j = \mathbf{I}_p, \quad \mathbf{J}_{NH} \mathbf{U}\mathbf{G} = \mathbf{U}\mathbf{G}$$

$$\text{where, } \underset{(NH \times q_j)}{\mathbf{Z}_j^H} = \begin{pmatrix} \mathbf{Z}_j \\ \vdots \\ \mathbf{Z}_j \end{pmatrix}, \quad \underset{(K \times p)}{\mathbf{G}} = \begin{pmatrix} \mathbf{G}_1 \\ \vdots \\ \mathbf{G}_H \end{pmatrix}, \quad (4)$$

$$\mathbf{U} = \text{b-diag}(\mathbf{U}_1, \mathbf{U}_2, \dots, \mathbf{U}_H) = \begin{pmatrix} \mathbf{U}_1 & \mathbf{0} & \cdots & \mathbf{0} \\ \mathbf{0} & \mathbf{U}_2 & \cdots & \mathbf{0} \\ \vdots & \vdots & \ddots & \vdots \\ \mathbf{0} & \mathbf{0} & \cdots & \mathbf{U}_H \end{pmatrix},$$

and $K = \sum_{h=1}^H K_h = \sum_{h=1}^H \sum_{s=1}^{r_s} K_{hs}$.

If we set $H = 1$ and define \mathbf{U}_H as a cluster indicator matrix for K_H clusters without the hierarchical clustering structure, that is, $\mathbf{U}_H = (u_{ik})$, ($i = 1, \dots, N$; $k = 1, \dots, K_H$) where $\sum_{k=1}^{K_H} u_{ik} = 1$ and $u_{ik} \in \{0, 1\}$, then (3) is equivalent to Cluster CA (van de Velden et al., 2017), which is equivalent to GROUPALS (Van Buuren & Heiser, 1989) when applied only to categorical variables.

Thus, MSCCA can be considered as an extension of Cluster CA that enables us to obtain the cluster allocation for each class simultaneously in a common low-dimensional space, in which quantifications for categories \mathbf{B}_j ($j = 1, \dots, m$) are optimally estimated for all clusters.

2.2 Algorithm

The parameters \mathbf{U} , \mathbf{G} and \mathbf{B}_j ($j = 1, \dots, m$) are estimated using the following alternating least squares algorithm. These updating formulas are obtained through a direct extension of cluster CA (van de Velden et al., 2017).

Step 1: Initialization. Determine K_{hs} ($h = 1, \dots, H$; $s = 1, \dots, r_h$) and p . Set the number of iterations to $t = 0$, and set a convergence criterion ε . Then, randomly generate initial clusters for each class.

Step 2: Updating \mathbf{B}_j . Let $\mathbf{B} = (\mathbf{B}'_1, \dots, \mathbf{B}'_m)'$ and $\mathbf{Z}^H = (\mathbf{Z}_1^H, \dots, \mathbf{Z}_m^H)$. Then find $\mathbf{B}^{(t+1)}$ as

$$\mathbf{B}^{(t+1)} = \sqrt{Nm} \mathbf{D}^{-1/2} \mathbf{B}^*$$

$$\text{where } \frac{1}{m} \mathbf{D}^{-1/2} \mathbf{Z}^{H'} \mathbf{J}_{NH} \mathbf{U}^{(t)} (\mathbf{U}^{(t)'} \mathbf{U}^{(t)})^{-1} \mathbf{U}^{(t)'} \mathbf{J}_{NH} \mathbf{Z} \mathbf{D}^{-1/2} = \mathbf{B} \mathbf{\Lambda} \mathbf{B}^{*'} \\ \mathbf{D} = \tilde{\mathbf{Z}}' \tilde{\mathbf{Z}}, \quad \tilde{\mathbf{Z}} = \text{b-diag}(\mathbf{Z}_1^H, \dots, \mathbf{Z}_m^H)$$

Step 3: Updating \mathbf{G} . Obtain $\mathbf{G}^{(t+1)}$ as follows.

$$\mathbf{G}^{(t+1)} = \frac{1}{m}(\mathbf{U}^{(t)'}\mathbf{U}^{(t)})^{-1}\mathbf{U}^{(t)'}\mathbf{J}_{NH}\mathbf{Z}\mathbf{B}^{(t+1)}$$

Step 4: Updating \mathbf{U} . $\mathbf{U}_h^{(t+1)}$ is obtained by updating by row. Specifically, each element in the i th row of \mathbf{U}_h , that is, $\mathbf{u}_{his} = (u_{hisk})$ ($k = 1, \dots, K_{hs}$), is updated as follows; if $v_{his} = 1$,

$$u_{hisk}^{(t+1)} = \begin{cases} 1 & (k = \arg \min_{\ell \in \{1, \dots, K_{hs}\}} \|\mathbf{f}_i - \mathbf{g}_{hs\ell}^{(t+1)}\|^2) \\ 0 & (\text{others}) \end{cases}$$

and otherwise $u_{hisk}^{(t+1)} = 0$. Here, \mathbf{f}_i is the i th row of $\mathbf{J}_N\mathbf{Z}\mathbf{B}^{(t+1)}$ and $\mathbf{g}_{hs\ell}^{(t+1)}$ is the cluster center of the k th cluster in the s th category in the h th supplementary variable.

Step 5: Convergence test Compute $\phi^{(t)}$, the value of the objective function (1) using updated parameters and for $t > 1$, if $\phi^{(t)} - \phi^{(t-1)} < \varepsilon$, terminate; otherwise, let $t = t + 1$ and return to Step 2.

2.3 Biplots

In this subsection, we consider how our MSCCA can be used to construct a biplot. In van de Velden et al. (2017), Cluster CA is formulated as a maximization problem. Using this, MSCCA in (3) can also be rewritten as the following maximization problem:

$$\begin{aligned} \max_{\mathbf{U}, \mathbf{B}} \psi(\mathbf{U}, \mathbf{B} | \mathbf{Z}^H) &= \text{tr } \mathbf{B}'\mathbf{Z}^{H'}\mathbf{J}_{NH}\mathbf{U}'(\mathbf{U}'\mathbf{U})^{-1}\mathbf{U}'\mathbf{J}_{NH}\mathbf{Z}^H\mathbf{B} \\ \text{s.t. } &\frac{1}{NHm} \sum_{j=1}^m \mathbf{B}_j'\mathbf{Z}_j^{H'}\mathbf{Z}_j^H\mathbf{B}_j = \mathbf{I}_p \end{aligned} \quad (5)$$

The proof for the equivalence between Equation (3) and (5) is provided in Proposition A.1 of Appendix A. With \mathbf{U} fixed, maximizing (5) is equivalent to minimizing

$$\min_{\mathbf{G}, \mathbf{B}} \phi^{CA}(\mathbf{G}, \mathbf{B} | \mathbf{Z}^H, \mathbf{V}, \mathbf{U}) = \|\tilde{\mathbf{P}} - \mathbf{D}_r^{1/2}\mathbf{G}\mathbf{B}'\mathbf{D}_c^{1/2}\|^2 \quad (6)$$

$$\text{s.t. } \frac{1}{Nm} \mathbf{B}'\mathbf{D}_c\mathbf{B} = \mathbf{I}_p$$

$$\text{where } \tilde{\mathbf{P}} = \mathbf{D}_r^{-1/2}(\mathbf{P} - \mathbf{r}\mathbf{c}')\mathbf{D}_c^{-1/2} \quad (7)$$

$$\mathbf{P} = (Nm)^{-1}\mathbf{U}'\mathbf{Z}^H, \quad \mathbf{r} = \mathbf{P}\mathbf{1}_Q, \quad \mathbf{c} = \mathbf{P}'\mathbf{1}_K, \quad \mathbf{D}_r = \text{diag}(\mathbf{r}), \quad \mathbf{D}_c = \text{diag}(\mathbf{c})$$

A proof of the equivalence between these objectives is given in van de Velden et al. (2017). Here, \mathbf{P} indicates a $(K \times Q)$ scaled contingency table of clusters for each class (row) and category (column), while each element in $\mathbf{r}\mathbf{c}'$, $r_k c_\ell$ ($k = 1, \dots, K$; $\ell = 1, \dots, Q$), indicates the scaled expected frequency under the assumption of independence between the k th cluster and the ℓ th category. Thus, the matrix $\tilde{\mathbf{P}}$ represents the standardized deviations from the independence assumption between cluster membership and the categorical variables.

From (6) it follows that the inner product of $D_r^{1/2}\mathbf{G}$ and $D_c^{1/2}\mathbf{B}$ approximates the matrix of standardized deviations from independence, $\tilde{\mathbf{P}}$. Hence, in MSCCA, \mathbf{G} and \mathbf{B} can be used to construct a biplot in which the larger the inner product of the k th row vector of \mathbf{G} and the ℓ th row vector in \mathbf{B} is, the stronger the association between the k th cluster and the ℓ th category tends to be.

2.4 Relationship to the linear row constraint approach

Takane and Hwang (2002) showed that several existing approaches for incorporating external information of individuals on an MCA biplot can be generalized into a linear row constraint framework.

To add linear row constraints in MCA, we can formulate the following objective function

$$\begin{aligned} \min_{\mathbf{G}, \mathbf{B}} \phi^{const}(\mathbf{G}, \mathbf{B} \mid \mathbf{Z}_j, \mathbf{V}_h) &= \frac{1}{Nm} \sum_{j=1}^m \|\mathbf{C}\mathbf{F} - \mathbf{Z}_j\mathbf{B}_j\|^2 \\ \text{s.t.} \quad &\frac{1}{Nm} \sum_{j=1}^m \mathbf{B}_j' \mathbf{Z}_j' \mathbf{Z}_j \mathbf{B}_j = \mathbf{I}_p, \quad \mathbf{J}_N \mathbf{C} \mathbf{F} = \mathbf{C} \mathbf{F} \end{aligned} \quad (8)$$

Here, \mathbf{C} is the $N \times N$ matrix containing the linear row constraints for the quantifications. If $\mathbf{C} = \mathbf{I}$, the problem reduces to the homogeneity formulation of MCA. The choice of \mathbf{C} depends on the objective of incorporating external information. For example, if one uses $\mathbf{C} = \mathbf{V}(\mathbf{V}'\mathbf{V})^{-1}\mathbf{V}'$, where $\mathbf{V} = \text{b-diag}(\mathbf{V}_1, \dots, \mathbf{V}_H)$, and we insert \mathbf{Z}_j^H for \mathbf{Z}_j , then (8) will amount to the averaging approach described in the introduction of our paper. That is, a class (category) is represented by the average quantification for the individuals corresponding to that class. Alternatively, if we aim to “remove” the effect of external information from a biplot, then we can use $\mathbf{C} = \mathbf{I} - \mathbf{V}(\mathbf{V}'\mathbf{V})^{-1}\mathbf{V}'$ (e.g., Takane & Shibayama, 1991; Takane & Hwang, 2002; Hwang & Takane, 2002). This amounts to deducting the class conditional means from data. For example, if as supplementary variable we have gender, the mean of all males is deducted from all male observations.

Although MSCCA follows a rather different approach to incorporate external information, we can reformulate the method in such a way that it does fit into the linear row constraint framework. In particular, for \mathbf{U} fixed, the MSCCA objective (3) can be rewritten as a minimization problem;

$$\begin{aligned} \min_{\mathbf{G}, \mathbf{B}} \phi^{MSCCA}(\mathbf{G}, \mathbf{B} \mid \mathbf{Z}, \mathbf{U}, \mathbf{V}) &= \frac{1}{NHm} \sum_{j=1}^m \|\mathbf{C}\mathbf{F} - \mathbf{Z}_j^H \mathbf{B}_j\|^2 \\ \text{s.t.} \quad &\frac{1}{Nm} \sum_{j=1}^m \mathbf{B}_j' \mathbf{Z}_j^{H'} \mathbf{Z}_j^H \mathbf{B}_j = \mathbf{I}_p, \quad \mathbf{J}_{NH} \mathbf{C} \mathbf{F} = \mathbf{C} \mathbf{F} \\ &\text{where } \mathbf{C} = \mathbf{U}(\mathbf{U}'\mathbf{U})^{-1}\mathbf{U}' \end{aligned} \quad (9)$$

$$\mathbf{U}_{(NH \times K)} = \text{b-diag}(\mathbf{U}_1, \mathbf{U}_2, \dots, \mathbf{U}_H), \quad \mathbf{Z}_j^H_{(NH \times q_j)} = \begin{pmatrix} \mathbf{Z}_j \\ \vdots \\ \mathbf{Z}_j \end{pmatrix}, \quad \mathbf{G}_{(K \times p)} = \begin{pmatrix} \mathbf{G}_1 \\ \vdots \\ \mathbf{G}_H \end{pmatrix},$$

Table 1: Name of categories in each variables of artificial data used for a simple illustration.

Variable type	Variable name	Category
Variables to estimate quantifications	Meal	Western, Asian
	Drink	Fruits juice, Tea, Alcohol
Supplementary variables	Nationality	American, Japense
	Gender	Male, Female

where, as before, \mathbf{U} has the hierarchical cluster structure constraint imposed by (2). From this formulation, it immediately follows that MSCCA can be considered as a special case of (8), with $\mathbf{C} = \mathbf{U}(\mathbf{U}'\mathbf{U})^{-1}\mathbf{U}'$. A proof of the equivalence between (8) and (9) is given in Proposition A.2 in Appendix A.

3 Numerical illustration of an MSCCA biplot

In this section, we present a small example, using artifical data, to illustrate how MSCCA works. In particular, by means of this example we zoom in on the differences between MSCCA and the averaging approach concerning the visualization of heterogeneous tendencies.

We first generate categorical data for 200 individuals. The generated data represent two categorical variables, meal and drink preference, and two supplementary variables, nationality and gender. The variables and corresponding categories are shown in Table 1. The aim of our analysis is to see whether there are different tendencies, with respect to the meal and drink preferences, for groups of individuals depending on their nationality and gender.

We generated the data in such a way that there are three true clusters in the full data set. Individuals in the first cluster choose “Western meal” for the meal variable, and “Fruit juice” for the drink variable (W&J), those in the second cluster choose “Asian meal” and “Tea” (A&T), and in the last cluster they choose “Western meal” and “Alcohol” (W&A). The frequency distribution of the generated artificial data over each cluster in each class is shown in Figure 1. As can be seen, there are two clusters for Americans, Asians and females and three clusters for the males.

The biplot resulting from the averaging approach is shown in Figure 2 (left). This plot clearly shows the overall tendencies of many Americans and Japanese; Americans and Japanese are strongly associated with W&J and A&T, respectively. However, due to the much smaller number of individuals choosing “Alcohol”, it is not possible to see who (i.e., which nationality or gender) chooses “Alcohol”.

In contrast, by obtaining clusters for each class, the tendencies of this relatively “small” number of individuals becomes visible in the MSCCA biplot (where we used the correct number of clusters for each class). Specifically, from the MSCCA biplot result shown in Figure 2 (right), we can clearly see that a small number of male Americans choose “Alcohol”. In addition, the MSCCA biplot still visualizes the tendencies of the larger

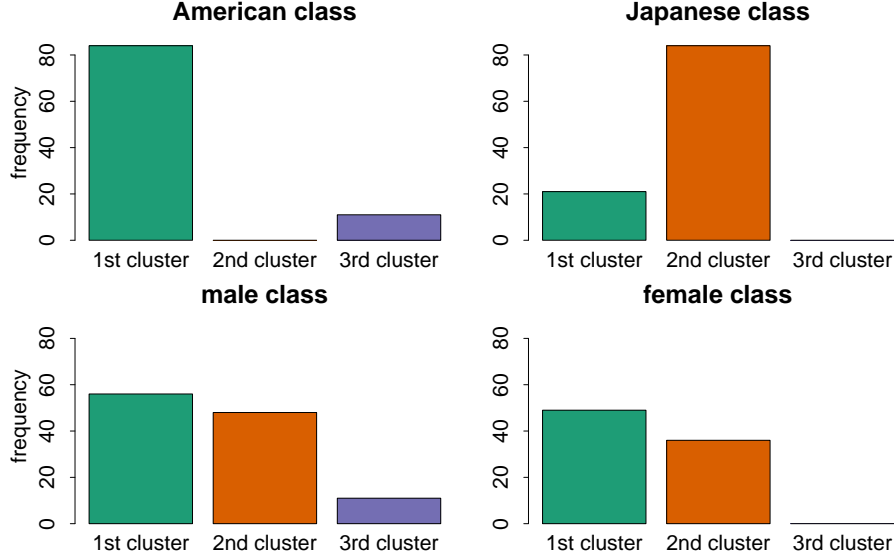


Figure 1: Frequency distributions for each combination of supplementary categories for each true cluster.

groups of individuals, as obtained in the averaging approach. Hence, MSCCA can show tendencies of small groups, without losing the information regarding the tendencies of larger groups.

In Appendix B, we provide, using the framework of CA, some additional insights into how (and when) the MSCCA and averaging approach differ with respect to the visualization of heterogeneous tendencies.

4 Simulation

In this section, we discuss the results of a simulation study that we conducted to evaluate the performance of MSCCA under different scenarios. In particular, using simulations we study the effects of the supplementary variables on the accuracy of clustering and biplots in MSCCA.

4.1 Data Generation

The data generation process can be divided into two steps, (i) generating an $N \times m$ data matrix and (ii) generating H supplementary variables.

(i) Generation of the data matrix.

We first divide the m variables into two groups, active variables; variables related to the clustering structure, and noise variables; variables unrelated to the cluster structure. Furthermore, we determine the cluster allocation using a multinomial distribution.

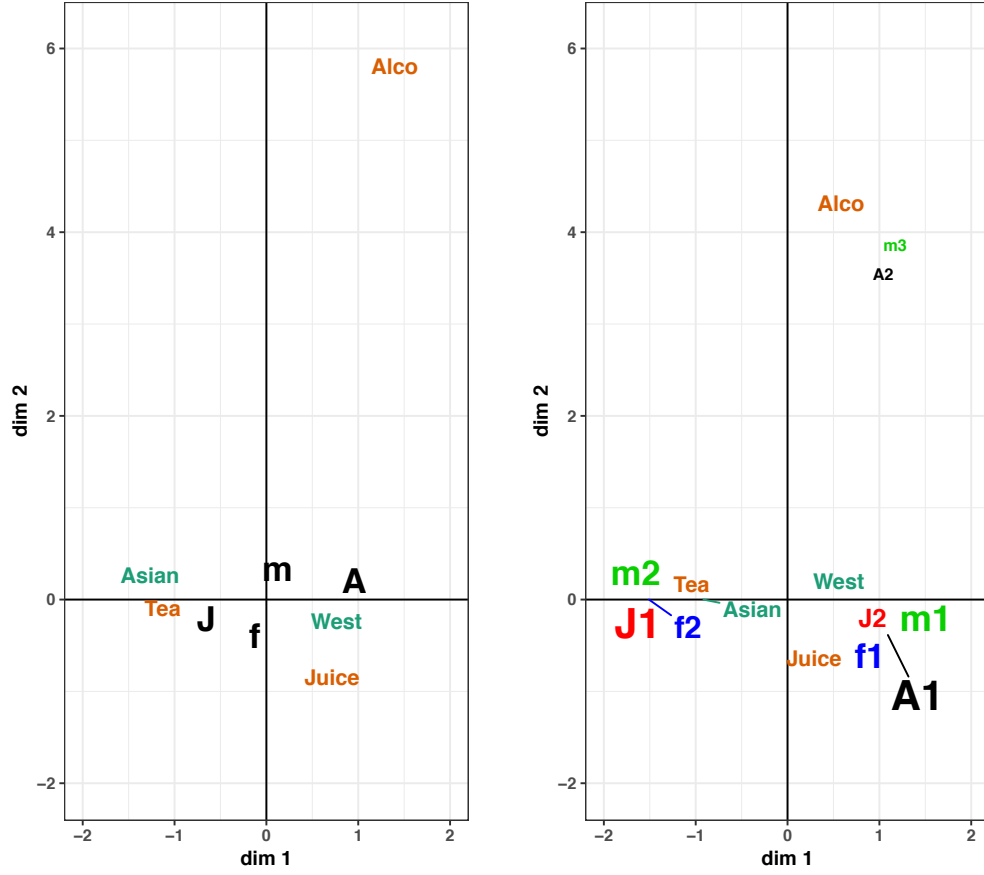


Figure 2: (Left) Results of the averaging approach. Average points are labelled “A” (American), “J” (Japanese), “m” (male), and “f” (female), label sizes correspond to class sizes. Other character labels indicate category points. (Right) Results of MSCCA. The points labelled “A,” “J,” “m,” or “f” followed by a number, correspond to the cluster points for each class.

We generate data for the active variables as follows. For each variable, one category is assigned a high probability: 0.8. The (low) probabilities assigned to the remaining categories are determined as $\bar{\mathbf{p}} = (\bar{p}_\ell)$ ($\ell = 1, \dots, q-1$), where $\bar{\mathbf{p}}$ is generated as $\bar{\mathbf{p}} = ((1 - 0.8) * (p_1, \dots, p_{q-1}) / \sum_{\ell=1}^{q-1} p_\ell)$ where $p_\ell \sim U(0, (1 - 0.8))$. The high probability categories are cluster specific.

To generate noise variables, we use a multinomial distribution in which the proportion for each category is $1/q$. In our simulation study, we set the ratio of active to noise variables as 1 : 1.

(ii) Generation of the data matrix corresponding to the supplementary variables.

In addition to an $N \times m$ data matrix, we generate data for H supplementary variables corresponding to two scenarios: balanced and unbalanced distributions over the categories. In the balanced scenarios, the multinomial probabilities for all categories are equal. In the unbalanced scenario, the probabilities are $1/S, \dots, r_h/S$, respectively, where r_h denotes the number of categories for the supplementary variable and $S = \sum_{s=1}^{r_h} s$.

4.2 Simulation study design

To assess the performance of the methods in different settings, we fix the number of observations $N = 300$ and the number of variables $m = 10$. Then, we consider a full factorial design with the number of categories for each variable $q = 5, 7$, the number of clusters $K = 2, 3$, the number of supplementary variables $H = 1, 3$, the number of categories for the supplementary variables $r_h = 3, 5$. Finally, for the supplementary variables we consider the balanced and unbalanced scenarios as described above.

For each combination of parameters in our simulation, we randomly generate 100 different $N \times m$ data matrices and $N \times H$ supplementary variable matrices. For each data set, we apply MSCCA using 500 random initial values.

4.3 Evaluation

We evaluate the performance of the methods using both the accuracy of the clustering and the biplots. For the clustering accuracy, we use the Adjusted Rand Index (ARI, Hubert & Arabie, 1985). The ARI assesses the similarity between two cluster allocations, taking the value one for a perfect recovery, with the value decreasing as the performance worsens. We calculate the ARI for the class specific clustering results separately.

For the biplot accuracy, we used a goodness of fit (GF) index for biplots (e.g., Gabriel, 2002). This GF index is equivalent to the so-called congruence coefficient (e.g., Lorenzo-Seva & Ten Berge, 2006). The GF between configurations \mathbf{Y} and \mathbf{H} is defined as,

$$\text{GF}(\mathbf{Y}, \mathbf{H}) = \frac{\text{tr}^2(\mathbf{Y}'\mathbf{H})}{\text{tr}(\mathbf{Y}'\mathbf{Y}) \text{tr}(\mathbf{H}'\mathbf{H})} = \cos^2(\mathbf{Y}, \mathbf{H}).$$

To assess the biplot accuracy, we calculate the GF between \mathbf{Y} and \mathbf{H} where $\mathbf{H} = \mathbf{GB}'$ (with \mathbf{G} and \mathbf{B} the MSCCA solutions) and $\mathbf{Y} = \tilde{\mathbf{P}}^{true} = \mathbf{D}_r(\mathbf{P}^{true} - \mathbf{rc}')\mathbf{D}_c$, where $\mathbf{P}^{true} = \mathbf{U}'\mathbf{Z}$

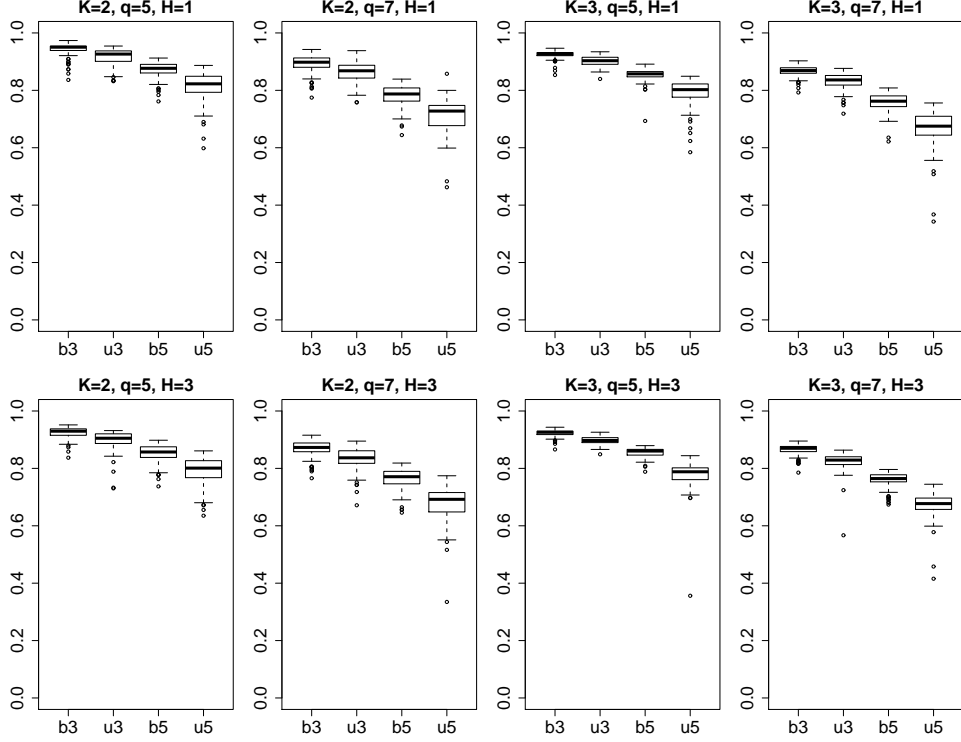


Figure 3: Boxplot of GF for each case. On the horizontal axis, “b3” indicates balanced categories in supplementary variables, and $r_h = 3$ for all $h = 1, \dots, H$, while “b5” has balanced categories with $r_h = 5$ for all h . Similarly, “u3” and “u5” indicate unbalanced categories with $r_h = 3, 5$, respectively.

and \mathbf{U} is the true cluster allocation. Note that by the definition, $\text{GF} \in [0, 1]$.

Note that, in our calculation of the GF index we assume that the true cluster allocation is known. In this way, the cluster accuracy does not affect the GF index.

4.4 Result

The results for the GF index are shown in Figure 3. We see that the GF tends to decrease as the number of categories q increases. The number of supplementary variables H does not appear to substantially affect the GF. The number of categories as well as whether the distributions over the categories of the supplementary variables are balanced or not, does appear to affect the GF. In particular, the GF tends to be better when there are fewer categories r_h in the supplementary variables and when the distributions over the categories is balanced.

The results concerning the cluster retrieval are shown in Figure 4. We see that, overall, the ARI tends to decrease when the number of clusters K increases and when the number of categories q decreases. On the other hand, the number of supplementary variables H and whether the distributions over the categories are unbalanced do not affect the median

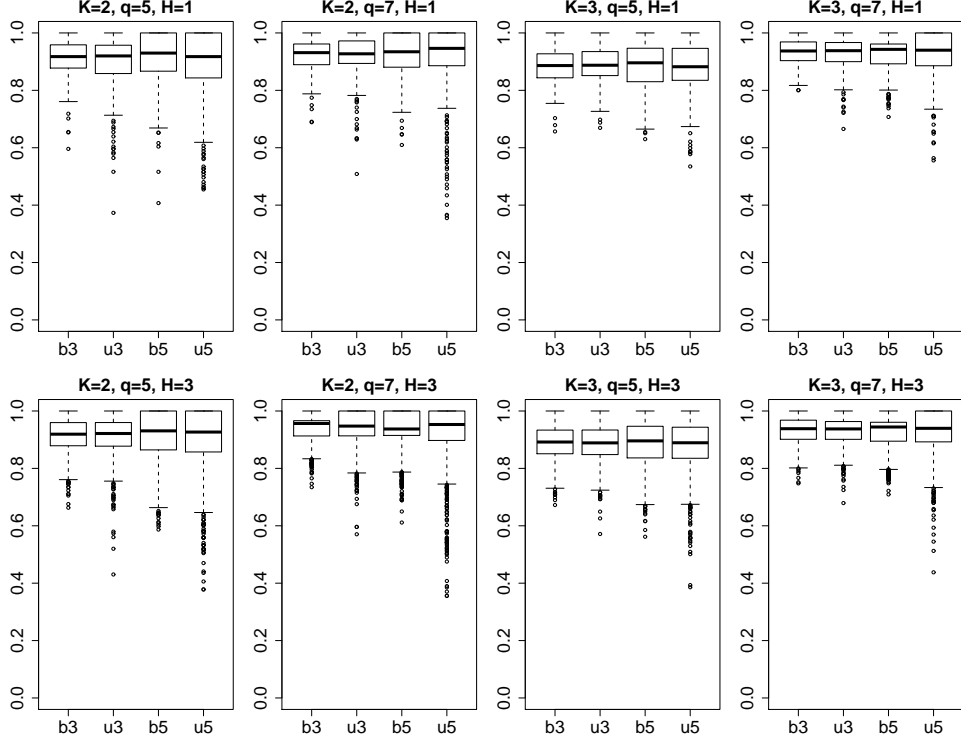


Figure 4: Boxplot showing the mean ARI for each case.

ARI substantially. However, we do see that for a larger number of supplementary variables with balanced distributions, there are more outlying results. In addition, the number of categories for the supplementary variables appears to affect the variances of the the ARI results. In particular, the ARI for $r_h = 5$ has greater variance than for $r_h = 3$.

4.5 Conclusions of the simulation study

The simulation study shows that the number of supplementary variables does not affect the accuracy of biplot and the clustering. This means that we can increase the number of supplementary variables H without this impacting the accuracy of the results. However, increasing the number of supplementary variables H leads to more points in the biplot, resulting in a more complicated visualization. Therefore, we can say that H can be increased as long as the biplot remains interpretable.

In addition, whereas the clustering results are hardly affected by the nature of the supplementary variables (i.e., the number of categories r_h , and whether the distribution over the categories is balanced or not), the results of the simulation study indicate that the biplot accuracy is. In particular, we see that using supplementary variables with more categories and unbalanced distributions over the categories, leads to a decrease in biplot accuracy.

In conclusion, when there are several candidates for supplementary variables, it is better

Table 2: Names of categories for each variable, and their corresponding label in biplots and descriptions.

Variable type	Variable name	Label	Description
Non-supplementary variables	Light conditions	Dark0	Daylight
		Dark1	Darkness: street lights present and lit
		Dark2	Darkness: street lights present but unlit
		Dark3	Darkness: no street lighting
	Weather conditions	Fine	Fine without high winds
		Rain	Raining without high winds
		Snow	Snowing without high winds
		Fine_w	Fine with high winds
		Rain_w	Raining with high winds
		Snow_w	Snowing with high winds
		Fog	Fog or mist if hazard
		Other	Other
	Road surface conditions	Dry	Dry
		Wet	Wet / Damp
		Snow	Snow
		Frost	Frost / Ice
		Flood	Flood (surface water over 3cm deep)
	Speed Limit	~30	Speed limit is up to 30km/h
		~70	Speed limit is up to 70km/h
Supplementary variables	Casualty class	Driver	Casualty is one driver
		Ped	Casualty is one pedestrian
	Area	Urban	Occurring in urban area
		Rural	Occurring in rural area

to select balanced supplementary variables with fewer categories.

5 Application

In this section, we illustrate the proposed method using a data set concerning road accidents in the United Kingdom. In particular, using these data, we would like to see how the circumstances in which a car accident occurs depends on the type of accident. We compare the results using MSCCA, the averaging approach, and Cluster CA, to see how the methods visualize the relationships.

5.1 Data and Setting

The data were obtained from the United Kingdom Department for Transport’s road safety statistics (<https://data.gov.uk/dataset/road-accidents-safety-data>). We selected data in which the observations are accidents and the (categorical) variables concern information regarding the accidents. Moreover, for this illustration, we selected accidents that occurred in January 2016 and that involved only one casualty, either a driver or a pedestrian, and for which at most two parties were involved. The resulting data set contains $N = 3,026$ observations.

For the circumstances of the accident, we consider four (i.e., $m = 4$) variables: Lighting condition, weather condition, road surface condition, and speed limit. Concerning the types of accident, we select two ($H = 2$) supplementary variables: Casualty class and area. A description of the variables and their categories can be found in Table 2.

As in any cluster analysis method, determining the number of clusters is not trivial. In MSCCA, the number of clusters must be pre-specified for each class K_{hs} ($h = 1, \dots, H; s = 1, \dots, r_h$). In this paper, we use the Krzanowski-Lai index (KL index, Krzanowski & Lai, 1988) to determine the number of clusters for each class, by doing separate cluster CA analyses. Specifically, we apply cluster CA to class specific data (that is, data corresponding to one category of the supplementary variables) to determine the number of clusters K_{hs} that corresponds to the optimal KL index.

This procedure results in four clusters for the driver class, five clusters for the pedestrian class, four in the urban class and four clusters for the rural class (i.e., $K_{11} = 4$, $K_{12} = 5$, $K_{21} = 4$ and $K_{22} = 4$). From here on, we refer to a cluster from the driver class as driver cluster, clusters from the pedestrian class are called pedestrian clusters, and so on.

To compare our results we also consider the averaging approach and cluster CA to the complete data (that is, including the supplementary variables in the analysis to determine clusters and quantifications). To select the number of clusters for the complete cluster CA analysis, we employed the KL index and obtained $K = 7$ clusters.

5.2 Result

5.2.1 MSCCA result

In the biplot for the MSCCA solution (Figure 5), we see that the largest pedestrian clusters, as well as the largest urban and rural clusters (P1, U1, and R1, respectively) are related to categories such as “Fine,” “Fine_w,” and “Dry.” This implies that many accidents that occur in urban and rural areas result in pedestrian casualties and have a strong association with what can generally be considered to be good driving conditions, such as fine weather and dry roads.

On the other hand, the largest driver cluster (D1) is related to categories such as “Dark3,” “Snow_w (weather condition),” and “Snow (road surface).” This indicates that many accidents that result in a driver casualty have a strong association with bad driving condition, such as a dark night or a slippery road. Note that there is also a driver cluster close to the good conditions, however, this is the smallest driver cluster, indicating that accidents resulting in a driver casualty are less likely to occur under good conditions.

In addition, for the rural class, even though the largest rural cluster is close to categories corresponding to good conditions, the second largest rural cluster is close to bad conditions, indicating that many accidents in rural areas occur in both good and bad conditions. Finally, the fourth-largest cluster for rural data and the third-largest clusters for the other classes, are in similar directions to the categories “Rain,” “Rain_w,” and, to some extent, “Wet.” This indicates that for all classes of the supplementary variables, there are clusters of accidents that occur in rainy weather.

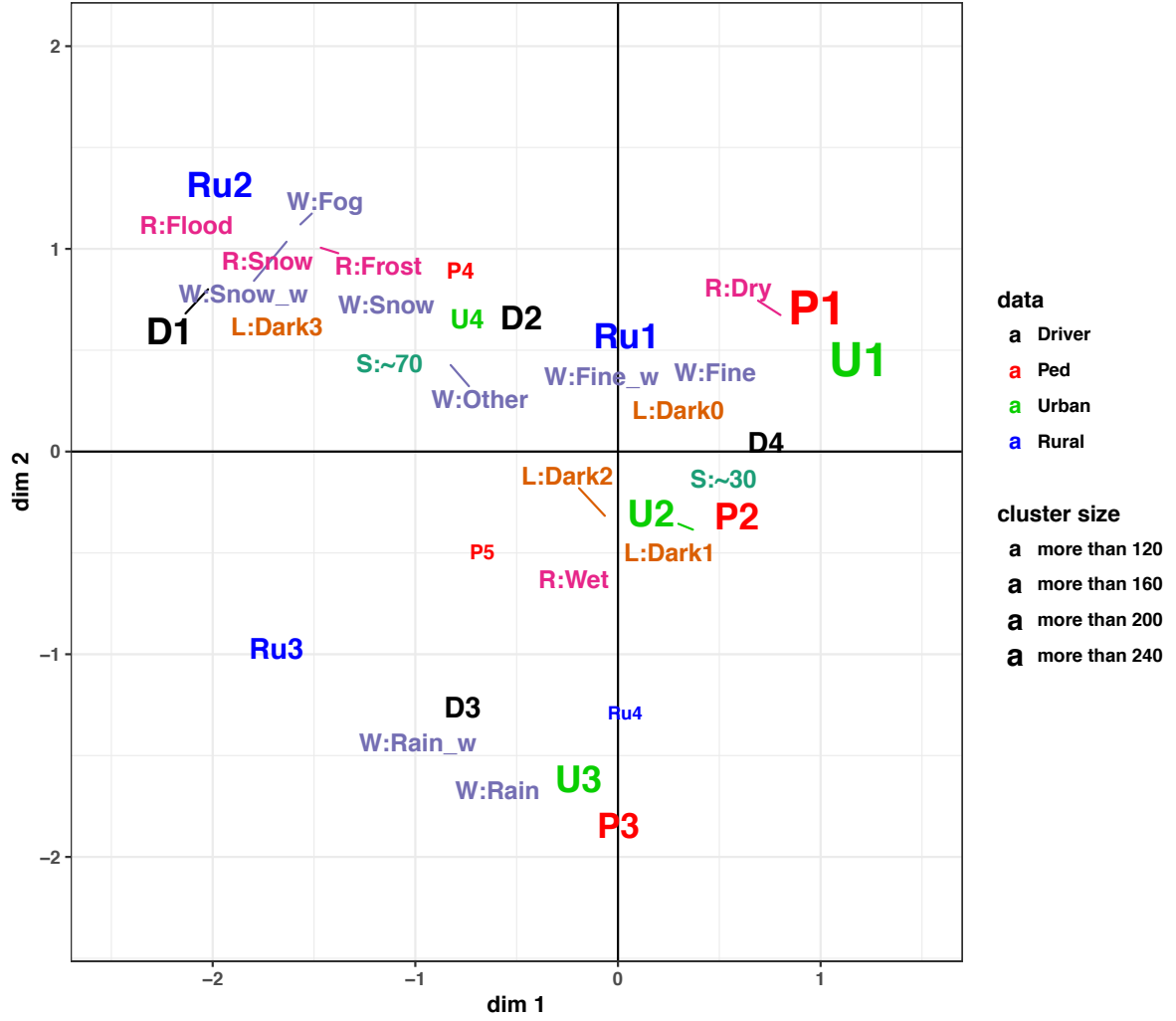


Figure 5: Results using MSCCA. The numbered labels indicate cluster points with “D” indicating the driver clusters, “P” corresponding to the pedestrian class, “U” to the urban class, and “Ru” to rural class clusters. The numbers are given according to the sizes among all clusters for a class (e.g., “D1” indicates the largest size cluster in a driver class), and the label sizes correspond to cluster sizes. Character labels beginning with “L”, “W”, “R” and “S” indicate category points for the variable of light, weather and road surface conditions, and speed limit, respectively.

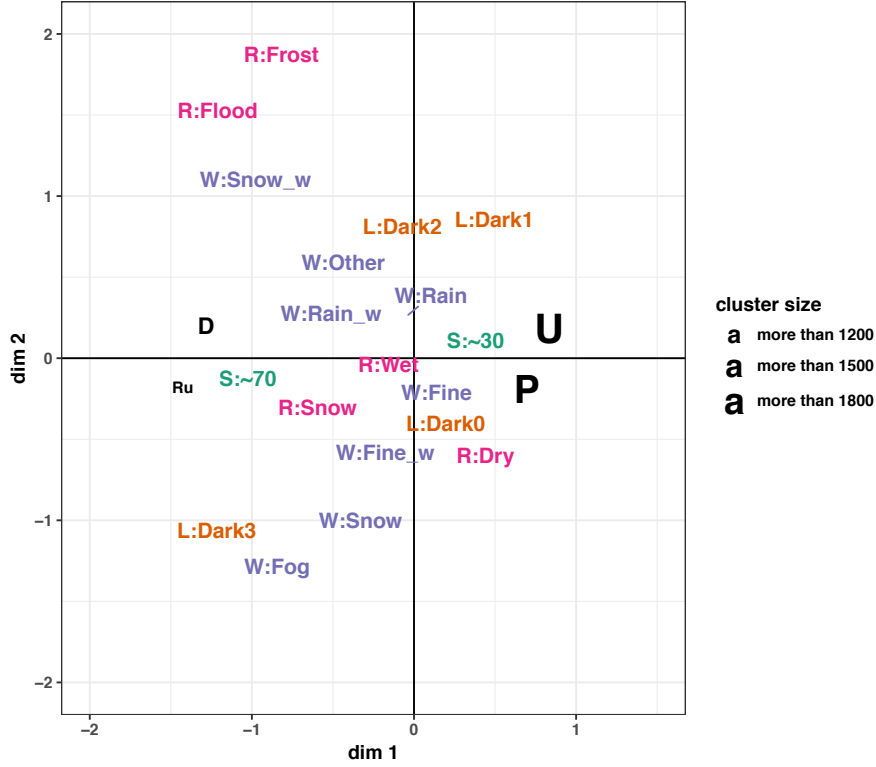


Figure 6: Results using the averaging approach. The character labels “D”, “P”, “U” and “Ru” indicate classes defined by supplementary variables, label sizes correspond to class sizes. Other character labels indicate category points, same as Figure 5.

By inspecting the MSCCA biplot and relating the class specific cluster points to the category quantifications, we can visually interpret how accidents, split out into different classes, relate differently to weather and road conditions. For example, we see that while for pedestrians, a sizable amount of accidents occur even in favorable conditions, accidents involving drivers are strongly related to bad conditions.

5.2.2 Averaging results

The results using the averaging approach are shown in Figure 6. We can still interpret the information regarding classes with respect to categories, but, due to the averaging of results, the information is limited. Specifically, we see that “Driver” and “Rural” are related to categories indicating bad conditions for driving (such as “~70” and “Show”), while “Pedestrian” and “Urban” are related to categories corresponding to good conditions (such as “~30”, “Fine,” and “Dark0”). However, it is difficult to interpret the relationship between

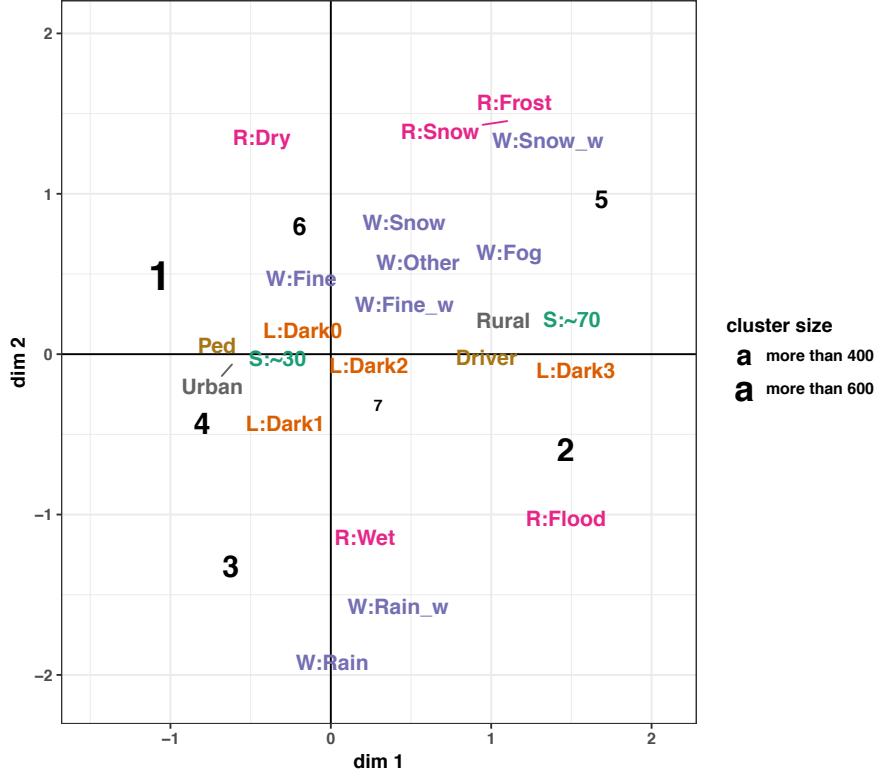


Figure 7: Results using cluster CA. Numbered labels indicate cluster points and the numbers are ordered according to the sizes of the clusters. Labeling of the other points is the same as in Figures 5 and 6.

classes and categories that are not close to the class quantifications. By averaging we can only interpret tendencies that many accidents in each class have in common. Differentiation with respect to smaller, but relatively homogeneous subgroups, is no longer possible.

5.2.3 Cluster CA result

Figure 7 shows the results using the Cluster CA approach. In contrast to the averaging approach, we can now distinguish different clusters corresponding to several accident tendencies. For example, there is a cluster associated with rain-related categories (such as “Rain” and “Wet”), whereas this relationship was not clear in the averaging result. However, in the Cluster CA approach, the interpretation with respect to classes is still limited. For example, we can see that “Pedestrian” and “Urban” are related to good conditions, but we cannot interpret the relationship between the “Pedestrian” and “Urban” class with conditions such as rainy and bad condition (e.g., “~70” and “Dark3”). In contrast, using

MSCCA, we can also interpret these relationship (e.g., we can see that the “Pedestrian” class appear to have a weaker association with bad condition than good and rainy condition, because the smallest pedestrian cluster is the closest to bad condition in MSCCA result.)

5.2.4 Conclusions of empirical data analysis

In summary, in this section we compared three visualization results to appraise differences in the biplots incorporation external information (i.e., class). All three methods enabled us to identify situations in which many accidents in each class occur. However, only by using MSCCA, we were able to differentiate between conditions in which many or few accidents occurred. Specifically, using this method, it became evident that relatively many accidents in the “Pedestrian” and “Urban” classes occur when conditions are good, and not so many when conditions are bad. Conversely, for the “Driver” class, accidents predominantly occur under bad conditions, with only few occurring when conditions are good. For accidents corresponding to the “Rural” class, it was found that they occur in both good and bad conditions. Finally, for all classes, we found relatively small clusters of accidents strongly related to rainy condition.

6 Conclusion

In this paper, we proposed a new approach to incorporate and interpret external information in a biplot for categorical data. Specifically, we introduced a multiple set extension to cluster CA, MSCCA, that makes it possible to visually interpret the relationship between external information and categories. In MSCCA, class specific clusters are obtained that make it possible to identify heterogeneous tendencies within each class. We showed that MSCCA can be related to the linear row constraint framework.

We investigated the performance of MSCCA under different conditions, by using a small simulation study. The results of this simulation showed that increasing the number of supplementary variables, H , has little effect on the cluster and biplot accuracies. However, results were better when supplementary variables with few categories and an even (balanced) distribution over the categories were used.

Our empirical analysis of road accident data showed that, while the averaging and Cluster CA approaches revealed only the tendencies corresponding to the majority of accidents in each class, the MSCCA biplot makes it possible to interpret heterogeneous tendencies within each class, regardless of cluster sizes.

Finally, it should be noted that MSCCA can also be used in different settings. In particular, MSCCA may also be applied in a three-way setting to visualize the relationship among multiple two-way datasets. For example, if we have $N \times m$ categorical datasets corresponding to T different time points, we can use MSCCA to visualize the relationships among clusters at different times.

A Proof

In this Appendix, several propositions regarding MSCCA are considered. Since MSCCA is an extension of cluster CA, without loss of generality, we only show the proof for cluster CA.

Proposition A.1. *Two optimization problems*

$$\begin{aligned} \min \phi(\mathbf{U}, \mathbf{G}, \mathbf{B} \mid \mathbf{Z}) &= \frac{1}{Nm} \sum_{j=1}^m \|\mathbf{U}\mathbf{G} - \mathbf{Z}_j \mathbf{B}_j\|^2 \\ \text{s.t.} \quad &\frac{1}{Nm} \sum_{j=1}^m \mathbf{B}_j' \mathbf{Z}_j' \mathbf{Z}_j \mathbf{B}_j = \mathbf{I}_p, \quad \mathbf{J}_N \mathbf{U} \mathbf{G} = \mathbf{U} \mathbf{G} \end{aligned} \quad (10)$$

and

$$\begin{aligned} \max \psi(\mathbf{U}, \mathbf{B} \mid \mathbf{Z}) &= \text{tr} \mathbf{B}' \mathbf{Z}' \mathbf{J}_N \mathbf{U}' (\mathbf{U}' \mathbf{U})^{-1} \mathbf{U}' \mathbf{J}_N \mathbf{Z} \mathbf{B} \\ \text{s.t.} \quad &\frac{1}{Nm} \sum_{j=1}^m \mathbf{B}_j' \mathbf{Z}_j' \mathbf{Z}_j \mathbf{B}_j = \mathbf{I}_p \end{aligned} \quad (11)$$

are equivalent.

Proof. At first the equivalence is shown when \mathbf{U} is fixed. Considering the constraints, Equation (10) can be rewritten as

$$\begin{aligned} \phi &= \frac{1}{Nm} \sum_{j=1}^m \|\mathbf{U}\mathbf{G} - \mathbf{Z}_j \mathbf{B}_j\|^2 \\ &= \frac{1}{Nm} \left(m \text{tr} \mathbf{G}' \mathbf{U}' \mathbf{U} \mathbf{G} - 2 \text{tr} \sum_{j=1}^m \mathbf{B}_j' \mathbf{Z}_j' \mathbf{U} \mathbf{G} + \text{tr} \sum_{j=1}^m \mathbf{B}_j' \mathbf{Z}_j' \mathbf{Z}_j \mathbf{B}_j \right) \\ &= \frac{1}{N} \text{tr} \mathbf{G}' \mathbf{U}' \mathbf{U} \mathbf{G} - \frac{2}{Nm} \text{tr} \mathbf{B}' \mathbf{Z}' \mathbf{U} \mathbf{G} + p \quad \left(\frac{1}{Nm} \sum_{j=1}^m \mathbf{B}_j' \mathbf{Z}_j' \mathbf{Z}_j \mathbf{B}_j = \mathbf{I}_p \right) \end{aligned}$$

Using $\mathbf{J}_N \mathbf{U} \mathbf{G} = \mathbf{U} \mathbf{G}$ and omitting the constant, this minimization will be

$$\frac{1}{N} \text{tr} \mathbf{G}' \mathbf{U}' \mathbf{U} \mathbf{G} - \frac{2}{Nm} \text{tr} \mathbf{B}' \mathbf{Z}' \mathbf{J}_N \mathbf{U} \mathbf{G} \quad (12)$$

Solving this for \mathbf{G} , we obtain

$$\mathbf{G} = \frac{1}{m} (\mathbf{U}' \mathbf{U})^{-1} \mathbf{U}' \mathbf{J}_N \mathbf{Z} \mathbf{B}$$

Inserting this in Equation (12), it will be

$$\begin{aligned} &\frac{1}{Nm^2} \text{tr} \mathbf{B}' \mathbf{Z}' \mathbf{J}_N \mathbf{U}' (\mathbf{U}' \mathbf{U})^{-1} \mathbf{U}' \mathbf{J}_N \mathbf{Z} \mathbf{B} - \frac{2}{Nm^2} \text{tr} \mathbf{B}' \mathbf{Z}' \mathbf{J}_N \mathbf{U}' (\mathbf{U}' \mathbf{U})^{-1} \mathbf{U}' \mathbf{J}_N \mathbf{Z} \mathbf{B} \\ &= -\frac{1}{Nm^2} \text{tr} \mathbf{B}' \mathbf{Z}' \mathbf{J}_N \mathbf{U}' (\mathbf{U}' \mathbf{U})^{-1} \mathbf{U}' \mathbf{J}_N \mathbf{Z} \mathbf{B} \end{aligned}$$

Minimizing this is equivalent to maximizing Equation (11). Next, the equivalence is shown when \mathbf{B} is fixed and \mathbf{U} is not. At first, a k -means type optimization problem

$$\min_{\mathbf{U}, \mathbf{G}} \|\mathbf{UG} - \mathbf{J}_N \mathbf{ZB}\|^2$$

is equivalent to the optimization problem in Equation (11), since this can be rewritten as

$$\begin{aligned} \|\mathbf{UG} - \mathbf{J}_N \mathbf{ZB}\|^2 &= \text{tr } \mathbf{G}' \mathbf{U}' \mathbf{UG} - 2 \text{tr } \mathbf{B}' \mathbf{Z}' \mathbf{J}_N \mathbf{UG} + \text{tr } \mathbf{B}' \mathbf{Z}' \mathbf{J}_N \mathbf{ZB} \\ &= - \text{tr } \mathbf{B}' \mathbf{Z}' \mathbf{J}_N \mathbf{U}' (\mathbf{U}' \mathbf{U})^{-1} \mathbf{U}' \mathbf{J}_N \mathbf{ZB} + \text{tr } \mathbf{B}' \mathbf{Z}' \mathbf{J}_N \mathbf{ZB} \end{aligned} \quad (13)$$

Here, we use $\mathbf{G} = m^{-1}(\mathbf{U}' \mathbf{U})^{-1} \mathbf{U}' \mathbf{J}_N \mathbf{ZB}$. Omitting a constant term, minimizing Equation (13) is equivalent to maximizing Equation (11). On the other hand, with \mathbf{B}_j ($j = 1, \dots, m$) fixed, Equation (10) can be written as

$$\begin{aligned} \sum_{j=1}^m \|\mathbf{UG} - \mathbf{Z}_j \mathbf{B}_j\|^2 &= \|\mathbf{UG} - \mathbf{ZB}\|^2 \\ &= \text{tr } \mathbf{G}' \mathbf{U}' \mathbf{UG} - 2 \text{tr } \mathbf{B}' \mathbf{Z}' \mathbf{J}_N \mathbf{UG} + \text{tr } \mathbf{B}' \mathbf{Z}' \mathbf{ZB} \\ &= - \text{tr } \mathbf{B}' \mathbf{Z}' \mathbf{J}_N \mathbf{U}' (\mathbf{U}' \mathbf{U})^{-1} \mathbf{U}' \mathbf{J}_N \mathbf{ZB} + \text{tr } \mathbf{B}' \mathbf{Z}' \mathbf{ZB} \end{aligned}$$

This is the same as Equation (13). Thus, we obtain the proposition. \square

Proposition A.2. *Minimizing Equation (10) with respect to \mathbf{B} is equivalent to minimizing*

$$\begin{aligned} \phi^{const}(\mathbf{B} | \mathbf{Z}, \mathbf{U}) &= \frac{1}{Nm} \sum_{j=1}^m \|\mathbf{CF} - \mathbf{Z}_j \mathbf{B}_j\|^2 \\ \text{s.t. } \frac{1}{Nm} \sum_{j=1}^m \mathbf{B}_j' \mathbf{Z}_j' \mathbf{Z}_j \mathbf{B}_j &= \mathbf{I}_p, \quad \mathbf{J}_N \mathbf{CF} = \mathbf{CF}, \quad \text{where } \mathbf{C} = \mathbf{U}(\mathbf{U}' \mathbf{U})^{-1} \mathbf{U}' \end{aligned} \quad (14)$$

Proof. Using constraints, Equation (14) can be rewritten as

$$\phi^{const} = \frac{1}{N} \text{tr } \mathbf{F}' \mathbf{CF} - \frac{2}{Nm} \text{tr } \mathbf{B}' \mathbf{Z}' \mathbf{J}_N \mathbf{CF} \quad (15)$$

Solving this for \mathbf{F} , we obtain

$$\mathbf{F} = \frac{1}{m} \mathbf{J}_N \mathbf{ZB}$$

Inserting this into Equation (15), we obtain a minimization problem of

$$-\frac{1}{Nm^2} \text{tr } \mathbf{B}' \mathbf{Z}' \mathbf{J}_N \mathbf{U} (\mathbf{U}' \mathbf{U})^{-1} \mathbf{U}' \mathbf{J}_N \mathbf{ZB}. \quad (16)$$

On the other hand, using the proof in Proposition A.1, the optimization problem in Equation (10) can also be rewritten as (16). Thus we obtain the proposition. \square

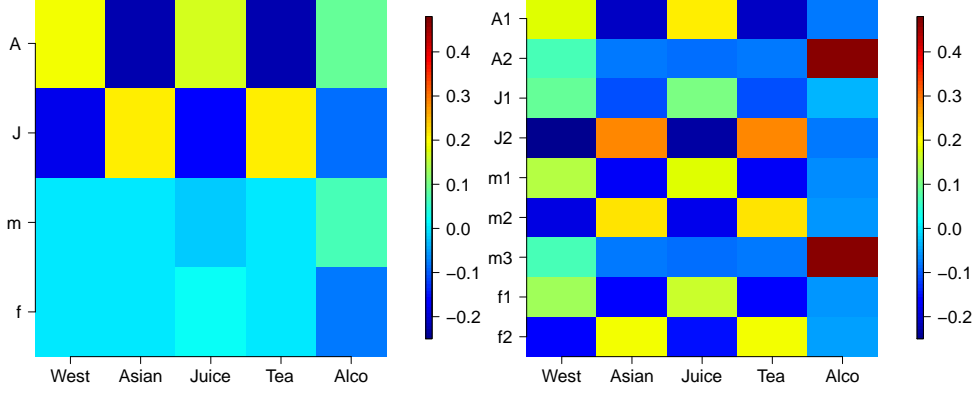


Figure 8: Heatmaps of $\tilde{\mathbf{P}}^{ave}$ (left) and $\tilde{\mathbf{P}}^{MSCCA}$ (right), respectively. These matrices are calculated as in (7), using $\mathbf{P}^{ave} = (NHm)^{-1}\mathbf{V}'\mathbf{Z}^H$ and $\mathbf{P}^{MSCCA} = (NHm)^{-1}\mathbf{U}'\mathbf{Z}^H$, respectively.

B How MSCCA compares to the averaging

In this Appendix, we investigate why MSCCA succeeds in clearly visualizing heterogeneous tendencies as compared to the averaging approach. To achieve this, we compare how associations between classes and categories are calculated using averaging and MSCCA.

Both MSCCA and averaging can be formulated within the CA framework. Averaging is equivalent to CA for the $\sum_{h=1}^H r_h \times Q$ contingency table (row is class, column is category), while MSCCA is equivalent to CA for the $\sum_{h=1}^H \sum_{s=1}^{r_h} K_{hs} \times Q$ contingency table (row is clusters in each class, column is category), for a given cluster allocation. Figure 8 shows heat maps of the relative deviations, $\tilde{\mathbf{P}}^{ave}$ and $\tilde{\mathbf{P}}^{MSCCA}$, with each method calculated based on their respective contingency tables. Thus, using this framework, we can say that the difference between the two methods is whether the rows of the contingency table are split by clusters in each class.

This factor causes a difference between averaging and MSCCA in how to calculate an expected frequency, $\mathbf{r}\mathbf{c}'$. Specifically, in the averaging approach, the expected frequency in the (3,1) element in $\tilde{\mathbf{P}}^{ave}$ is calculated using the number of individuals *who are American* and choose “Alcohol,” while the one in the (2,5) element in $\tilde{\mathbf{P}}^{MSCCA}$ is calculated using the number of individuals *who are in the second cluster in the American class* and choose “Alcohol.” That is, in MSCCA, the number of individuals used for calculating expected frequency is less for each row in the contingency table than the number for the averaging approach.

Note that the relative deviation indicates how large the observed frequency (i.e., the number of individuals choosing a particular category) is, compared to the expected frequency (i.e., the expected number of individuals choosing the category under the assumption of independence). Therefore, the relative deviation tends to increase when the expected frequency is calculated using the limited number of individuals who select the same categories.

Thus, in MSCCA, clustering individuals for each class enables us to see clearly the heterogeneous tendencies within each class, regardless of the size of groups having a similar tendency.

References

- Böckenholt, U., & Böckenholt, I. (1990). Canonical analysis of contingency tables with linear constraints. *Psychometrika*, 55(4), 633–639.
- Böckenholt, U., & Takane, Y. (1994). Linear constraints in correspondence analysis. In M. Greenacre & J. Blasius (Eds.), *Correspondence analysis in social sciences* (pp. 112–127). London: Academic Press.
- Friendly, M. (1999). Extending mosaic displays: Marginal, conditional, and partial views of categorical data. *Journal of Computational and graphical Statistics*, 8(3), 373–395.
- Gabriel, K. R. (2002). Goodness of fit of biplots and correspondence analysis. *Biometrika*, 89(2), 423–436.
- Gower, J. C., & Hand, D. J. (1996). *Biplots*. London: Chapman & Hall.
- Greenacre, M. (1993). Biplots in correspondence analysis. *Journal of Applied Statistics*, 20(2), 251–269.
- Greenacre, M. (2013). Contribution biplots. *Journal of Computational and Graphical Statistics*, 22(1), 107–122.
- Greenacre, M. J. (1984). *Theory and applications of correspondence analysis*. London: Academic Press.
- Hubert, L., & Arabie, P. (1985). Comparing partitions. *Journal of classification*, 2(1), 193–218.
- Hwang, H., Dillon, W. R., & Takane, Y. (2006). An extension of multiple correspondence analysis for identifying heterogeneous subgroups of respondents. *Psychometrika*, 71(1), 161–171.
- Hwang, H., & Takane, Y. (2002). Generalized constrained multiple correspondence analysis. *Psychometrika*, 67(2), 211–224.
- Hwang, H., Yang, B., & Takane, Y. (2005). A simultaneous approach to constrained multiple correspondence analysis and cluster analysis for market segmentation. *Asia Pacific Advances in Consumer Research*, 6, 197–199.
- Krzanowski, W. J., & Lai, Y. (1988). A criterion for determining the number of groups in a data set using sum-of-squares clustering. *Biometrics*, 44(1), 23–34.
- Lorenzo-Seva, U., & Ten Berge, J. M. (2006). Tucker’s congruence coefficient as a meaningful index of factor similarity. *Methodology*, 2(2), 57–64.
- Takane, Y., & Hwang, H. (2002). Generalized constrained canonical correlation analysis. *Multivariate Behavioral Research*, 37(2), 163–195.
- Takane, Y., & Shibayama, T. (1991). Principal component analysis with external information on both subjects and variables. *Psychometrika*, 56(1), 97–120.
- Takane, Y., Yanai, H., & Mayekawa, S. (1991). Relationships among several methods of linearly constrained correspondence analysis. *Psychometrika*, 56(4), 667–684.

- Theus, M., & Lauer, S. R. (1999). Visualizing loglinear models. *Journal of Computational and Graphical Statistics*, 8(3), 396–412.
- Van Buuren, S., & de Leeuw, J. (1992). Equality constraints in multiple correspondence analysis. *Multivariate behavioral research*, 27(4), 567–583.
- Van Buuren, S., & Heiser, W. J. (1989). Clustering n objects into k groups under optimal scaling of variables. *Psychometrika*, 54(4), 699–706.
- van de Velden, M., D’Enza, A. I., & Palumbo, F. (2017). Cluster correspondence analysis. *Psychometrika*, 82(1), 158–185.
- Yanai, H. (1986). Some generalizations of correspondence analysis in terms of projectors. In E. Diday, Y. Escoufier, L. Lebart, J. E. Pages, Y. Schektman, & R. Thomassone (Eds.), *Data analysis and informatics IV* (pp. 193–207). Amsterdam: North Holland.
- Yanai, H. (1988). Partial correspondence analysis and its properties. In C. Hayashi, M. Jambu, E. Diday, & N. Ohsumi (Eds.), *Recent developments in clustering and data analysis* (pp. 259–266). Boston: Academic Press.
- Yanai, H., & Maeda, T. (2002). Partial multiple correspondence analysis. In S. Nishisato, Y. Baba, H. Bozdogan, & K. Kanefuji (Eds.), *Measurement and Multivariate Analysis* (pp. 57–68). Tokyo: Springer.